NASA/TM-2020-5003983

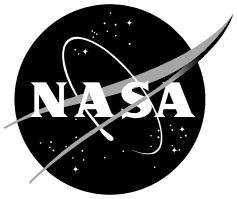

The Influence of Acid Group Clustering on the Thermal and Mechanical Properties of a Self-Healing Polymer

Keith L. Gordon, Kristopher E. Wise, and Emilie J. Siochi
Langley Research Center, Hampton, Virginia

Kevin R. Hadley
National Institute of Aerospace, Hampton,Virginia

July 2020

NASA STI Program ... in Profile

Since its founding, NASA has been dedicated to the advancement of aeronautics and space science. The NASA scientific and technical information (STI) program plays a key part in helping NASA maintain this important role.

The NASA STI program operates under the auspices of the Agency Chief Information Officer. It collects, organizes, provides for archiving, and disseminates NASA's STI. The NASA STI program provides access to the NTRS Registered and its public interface, the NASA Technical Reports Server, thus providing one of the largest collections of aeronautical and space science STI in the world. Results are published in both non-NASA channels and by NASA in the NASA STI Report Series, which includes the following report types:

- TECHNICAL PUBLICATION. Reports of completed research or a major significant phase of research that present the results of NASA Programs and include extensive data or theoretical analysis. Includes compilations of significant scientific and technical data and information deemed to be of continuing reference value. NASA counterpart of peer-reviewed formal professional papers but has less stringent limitations on manuscript length and extent of graphic presentations.

- TECHNICAL MEMORANDUM. Scientific and technical findings that are preliminary or of specialized interest, e.g., quick release reports, working papers, and bibliographies that contain minimal annotation. Does not contain extensive analysis.

- CONTRACTOR REPORT. Scientific and technical findings by NASA-sponsored contractors and grantees.

- CONFERENCE PUBLICATION. Collected papers from scientific and technical conferences, symposia, seminars, or other meetings sponsored or co-sponsored by NASA.

- SPECIAL PUBLICATION. Scientific, technical, or historical information from NASA programs, projects, and missions, often concerned with subjects having substantial public interest.

- TECHNICAL TRANSLATION. English-language translations of foreign scientific and technical material pertinent to NASA's mission.

Specialized services also include organizing and publishing research results, distributing specialized research announcements and feeds, providing information desk and personal search support, and enabling data exchange services.

For more information about the NASA STI program, see the following:

- Access the NASA STI program home page at http://www.sti.nasa.gov

- E-mail your question to help@sti.nasa.gov

- Phone the NASA STI Information Desk at 757-864-9658

- Write to:
  NASA STI Information Desk
  Mail Stop 148
  NASA Langley Research Center
  Hampton, VA 23681-2199

NASA/TM-2020-5003983

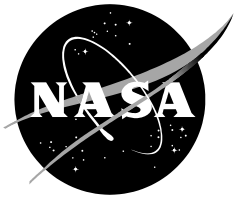

The Influence of Acid Group Clustering on the Thermal and Mechanical Properties of a Self-Healing Polymer

Keith L. Gordon, Kristopher E. Wise, and Emilie J. Siochi
Langley Research Center, Hampton, Virginia

Kevin R. Hadley
National Institute of Aerospace, Hampton, Virginia

National Aeronautics and
Space Administration

Langley Research Center
Hampton, VA 23681

July 2020

Available from:

NASA STI Program / Mail Stop 148
NASA Langley Research Center
Hampton, VA 23681-2199
Fax: 757-864-6500

The Influence of Acid Group Clustering on the Thermal and Mechanical Properties of a Self-Healing Polymer

Abstract

To better understand the molecular level mechanisms behind the self-healing of polymer systems, this work developed and validated a molecular dynamics model for a self-healing polymer, Surlyn® 8940. The polymer chains were built using free-radical polymerization between ethylene monomers (~95 mol %) and methacrylic acid monomers. Predicted thermal and structural properties including thermal conductivity, heat capacity, transition temperatures, thermal expansion coefficient, density, and Young's modulus were shown to be in good agreement with experimental values. Furthermore, the effects of cluster formation among the acid groups on these properties were explicitly explored.

INTRODUCTION

System reliability is critical in aerospace systems where accomplishing a mission is directly dependent upon retention of structural integrity. Self-healing materials provide a route for increasing damage tolerance and enhancing reliability while also minimizing the time and effort required for repairs. In recent years, many strategies and materials have been developed and studied to enable self-healing in structures and materials.[1] Current self-healing strategies are categorized as either passive or active and either limited or repeatable.

Significant attention has been paid to a passive self-healing strategy in which polymer-filled capsules,[2] hollow fibers,[3] or micro-vascular channels[2e] are embedded into host materials in locations where cracks are expected to occur.[4] Upon crack formation and propagation, the capsules rupture and their contents fill in the void to "heal" the host material and prevent catastrophic failure. Because the repair material is depleted during the process, this strategy is not appropriate for conditions where damage may occur more than once.

Other self-healing materials can be molecularly designed to repeatedly heal, but usually require a stimulus to activate the healing process after the damage event. In some composite materials, heat is applied to a damaged site to allow the matrix material to flow and reseal the damage site.[4-5] Similarly, application of heat can be used to drive reversible Diels-Alder reactions to form chemical cross-links between polymers.[6] Compressive mechanical force is sufficient for healing in some supramolecular materials, such as polymers containing strong hydrogen-bonding end groups developed by Leibler and co-workers.[7]

In contrast, the applications which motivate the present work require self-healing materials that are capable of repeated, autonomous, and rapid damage recovery.[8] The puncture healing DuPont Surlyn® 8940 and Nucrel® polymers are examples of this class of materials. They are capable of sealing ballistic induced damage within microseconds of the puncture event.[8a] Of the ballistic self-healing polymers in the literature, Surlyn® 8940 exhibits the highest healing efficacy.[8a, 8c]

Surlyn® 8940 is a random copolymer mixture of ethylene (94.6 mol%) and methyl acrylic acid (5.4 mol%). After radical polymerization of the monomers at high temperature and pressure, the polymer is treated with highly concentrated NaOH to neutralize 30% of the acid groups. Other Surlyn® 8940 derivatives exist with differing amounts of ethylene and extent of ionization. Nucrel®, for example, has the same molar composition as Surlyn® 8940, but all of its acid groups are protonated. A common characteristic of all ballistic self-healing polymers is the existence of an order/disorder transition temperature (T_o), which is found between the glass transition temperature (T_g) and the melting temperature (T_m).[8b] In differential scanning calorimetry (DSC) measurements, a peak is observed at T_o in the pristine material, but is lost after the polymer is heated past T_m. The peak is recovered only after an equilibration period of approximately 24 hours.[8b]

While some experimental ambiguity about the detailed damage processes occurring in these materials remains,[8] the penetration event is primarily understood to be an elastic deformation. A combination of

bulk elastic recovery, polymer re-entanglement, and the reformation of ionic bonds causes the material to return to its original shape after a recovery period. The experimental data suggest that material heating in the zone around the puncture site makes the polymer chains sufficiently mobile to re-entangle, and for the ionic or acidic functional groups to reform into clusters. High-speed video evidence suggests a shock wave precedes the penetrator in reaching the exit side of the sample.[8a] In either case, a small fraction of the deformed material is lost, with the majority elastically recovering the initial shape.

Many of the details of the recovery process are dependent on the physical and chemical properties of the particular material under investigation,[8c-e] the details of the test method,[8b, 8e] and the environmental conditions under which the test is performed.[8c, 8e] The most important material characteristics are polymer backbone flexibility and the presence of side chain functional groups capable of forming clusters, although the self-healing behavior of the fully protonated polymer Nucrel® shows that these functional groups need not be ionic.[8a, 8c] Aggregation of cluster forming groups can be enhanced by blending additives into the material,[8c] although additive concentration must be limited to avoid loss of self-healing behavior. While this effect is not fully understood, it appears that the additive may be acting as both a plasticizer for the chain backbone and a cluster-promoting agent. This would explain the effect of adding oxalic acid, which significantly improves healing behavior while simultaneously reducing elastic modulus.[8d]

The key difference among different test methods is the generation of heat at the damage site. Both sawing-induced damage and ballistic penetration result in self-healing, although in the latter case this behavior is relatively insensitive to details like bullet size and velocity.[8e] Low velocity punctures and clean cuts by a sharp blade, on the other hand, do not self-heal. Finally, the primary environmental condition which must be controlled is temperature. In order for healing to occur, the ambient temperature must be above the glass transition temperature, to enable chain mobility and re-entanglement, but below the order-disorder transition, above which the acid group clustering is greatly diminished.[8b] Elastic

recovery will still occur above the order-disorder transition, up to the melting temperature, but the mechanical properties of the polymer will reduced due to the limited reformation of acid group clusters.

This brief overview shows that there is broad understanding of many qualitative details of self-healing, but a more comprehensive quantitative framework is lacking. Rational design of application tailored self-healing materials will require a better understanding of the relationship between molecular-scale structural and chemical details of the material and its macroscopic properties and behavior. This work describes some initial steps in this direction, including the development of an atomistic model for Surlyn® 8940 and the use of molecular dynamics simulations to predict a number of thermal and mechanical properties relevant to self-healing. The performance of this model has been assessed by validating the simulation results against experimental data. Specifically, the model has been validated by comparing predicted density, Young's modulus, heat capacity, thermal expansion coefficient, transition temperatures, and thermal conductivity to experimental measurements. This paper lays the groundwork for future efforts to understand the structure-property relationships for this class of material.

EXPERIMENTAL

Surlyn® 8940 samples, provided by Dupont, had an average thickness of 0.6386 cm and were used as received. Its monomeric structure and molar composition can be seen in Figure 1. A NETSCH Heat Flow Meter (HFM) 436 Lambda was utilized to measure thermal conductivity of Surlyn® 8940 polymer. A NETZSCH thermal mechanical analyzer (TMA) was used to acquire thermal expansion coefficients. A static load of 20 cN was applied while the polymers were heated at a rate of 20 K/min over a temperature range of 283 K to 353 K. A 10-minute isothermal hold at 283K was applied at the beginning of each run.

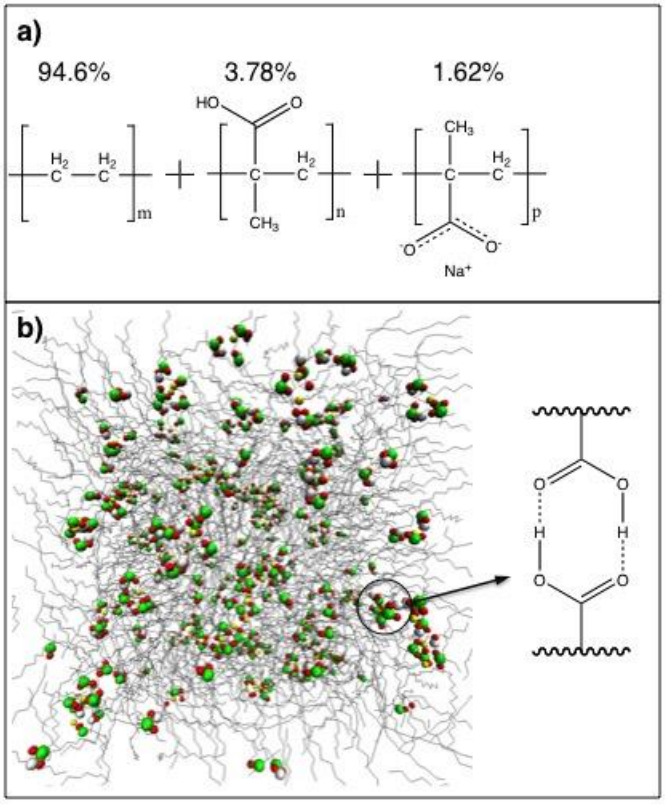

Figure 1. Composition of monomers in Surlyn® 8940 (a). Snapshot of equilibrated polymer model with clusters of dimers highlighted (b). Backbone carbons are represented by lines, carbonyl carbons are represented by green spheres, oxygens by red spheres, hydrogens by white spheres and sodium ions by yellow spheres.

SIMULATION DETAILS

All simulations were performed with the LAMMPS (Large-scale Atomic/Molecular Massively Parallel Simulator).[9] After the polymer system was built using the procedure described in the following section, equilibration simulations of various durations were run with a time step of 1.0 fs using the Nosé-Hoover barostat and thermostat to maintain the pressure and temperature in an isothermal-isobaric (NPT) ensemble at 298 K and 1.0 bar.[10]

After the equilibration, simulations were run to measure Young's modulus, transition temperatures, heat capacity, thermal expansion coefficient, thermal conductivity, and viscosity. For Young's modulus, the length of the simulation cell was increased in the desired direction at a strain rate of 1% per 1 ns over the course of 5 ns. The results from all three directions were averaged and are reported below.

Heat capacity and thermal expansion coefficient were calculated from enthalpy, temperature, and volume measurements taken from three NPT simulations at 290 K, 300 K, and 310 K at a constant pressure of 1.0 bar via equations (1) and (2):

$$C_P = \left(\frac{\partial H}{\partial T} \right)_P \approx \left(\frac{H_2 - H_1}{T_2 - T_1} \right) \tag{1}$$

$$a = \left(\frac{\partial \ln V}{\partial T} \right)_P \approx \left(\frac{\ln V_2 - \ln V_1}{T_2 - T_1} \right) \tag{2}$$

In equation (1), C_P represents heat capacity and H_x is the average enthalpy of the system at temperature T_x. In equation (2), α represents thermal expansion coefficient and V_x is the average molar volume at temperature T_x.[11]

The transition temperatures were determined by running the equilibrated system at a series of 21 temperatures between 100 and 450 K with a 1 ns equilibration period and a 1 ns data collection period at each temperature. The system was initially annealed to 100 K, equilibrated, and run at that same temperature. The end configuration served as the initial configuration for the next higher temperature simulation and this cycle was repeated until all 21 simulations were completed. Phase change temperatures were identified by significant changes in slope in the density versus temperature plots.

Thermal conductivity and viscosity were measured using the reverse non-equilibrium molecular dynamics (RNEMD) method developed by Müller-Plathe and co-workers.[12] In these simulations the atoms are divided into a number of slabs, N, and the kinetic energy of the hottest atom in slab N is exchanged with the kinetic energy of the coldest atom in slab N/2 over the course of 5 ns. This induces a smooth thermal gradient where slab N/2 will be the hottest and slab N will be the coldest. The thermal

conductivity can subsequently be measured from the slope of this gradient. A comparable procedure is used for the calculation of viscosity, but the x-components of velocities are exchanged instead of atomic kinetic energies. Alternative approaches, such as SLLOD could not be used because of their inability to include long-range Coulombic interactions.[12]

POLYMER CONSTRUCTION

For predominantly (~95 mol%) aliphatic hydrocarbon polymers such as Surlyn® 8940, substantial gains in computational efficiency can be realized at little cost in fidelity by utilizing a united atom model for the CHx repeat units and the methyl groups of the methacrylic acid monomers. The DREIDING force field, known to be accurate and efficient in modeling related polymer systems,[13] was utilized for the bonded and non-bonded interactions for the united atom sites in this work. The carboxylic acid sites, however, require explicit representation of all atoms to reliably model the physical interactions believed to be essential in the behavior of Surlyn® 8940. While mixing of force field parameters is generally undesirable, the lack of reliable charges for the acid groups in the DREIDING forcefield required the adoption of alternative parameters. In this work, atomic charges and van der Waals (vdW) parameters for these groups were taken from the Charmm General Force Field (CGenFF)[14] because of its demonstrated success in modeling the dimerization of carboxylic acid groups.[15]

Polymer chains of Surlyn® 8940, with the same stoichiometry as the experimental samples, were built using a free-radical polymerization technique inspired by the work of Perez *et al*[16] and Farah *et al*.[17] To begin, 5000 monomers, in the appropriate molar ratios, were randomly placed on a grid in a cubic cell with 70 Å long sides and equilibrated during a 1.0 ns simulation at 500 K and 1350 bar. Radial distribution functions (RDFs) were measured in the equilibrated simulation cell to determine an appropriate interaction distance between potentially reactive sites. This separation, 5.5 Å, was used as the reaction cutoff distance in subsequent polymerization simulations. Some modifications to the methods described in the literature[16-17] were found to improve the polymer structures and promote entanglement.

First, at points in the polymerization where no monomers were within reaction distance, the repulsive interactions between monomers and polymer chains were softened, the interaction between monomers and reactive sites were strengthened, and the radius of the reaction shell was increased. This accelerated the polymerization by allowing the monomers to move past intervening chains to reach reactive sites more quickly. In addition, the polymerization process was continued until all monomers had reacted, rather than discarding unreacted monomers after some arbitrary number of steps. Trial simulations revealed an initial population of 66 reactive monomers provided acceptable agreement with experimental values for polydispersity and radii of gyration without exceeding available computational resources.

The initial 66 reactive monomers were chosen at random from the full equilibrated system of 5000 monomers. Once a reactive monomer formed a bond with the closest monomer within the reaction cutoff distance, the new bond was assigned a force constant of 300 kcal/mol and an equilibrium distance of 2.50 Å. This softer bond interaction and longer bond length limits the large forces that would be found with standard carbon-carbon bond parameters at the non-equilibrium geometry found immediately after bond formation. The system was equilibrated for 500 fs at 298 K and 1350 bar with these parameters, after which the force constant and equilibrium distance of 350 kcal/mol and 1.53 Å respectively, were switched to the normal values found in the DREIDING force field.[13] Upon reversion to the DREIDING bond forces, the system was equilibrated for another 500 fs. This process was repeated until no monomers reacted for 10 cycles, whereupon the vdW interactions were altered as described earlier and a short simulation, typically less than 1000 fs, was run until monomers were within reactive distance of a reactive monomer. The vdW interactions were then returned to their original values and the algorithm continued.

After the polymer chains were built, the reactive groups were converted to terminal methyl carbons and the system pressure was reduced from 1350 bar to 1.0 bar at a constant rate during a 0.5 ns simulation. This was followed by another 0.5 ns equilibration simulation at 1.0 bar. At this point, 30% of the carboxylic acid groups were randomly selected to be ionized, thus converting the polymer system from Nucrel® to Surlyn® 8940. The 81 carboxylic groups were converted to carboxylates by removing the O-H bond, replacing the hydrogen atom with a sodium ion, and modifying the charge distribution. A short

run to relax high-energy configurations in the modified system was followed by a 1.0 ns equilibration run. The final cubic unit cell had a side length of 65.5Å. The simulation cells prepared in the manner described above will be referred to as “baseline” throughout this paper.

Several modified systems were also prepared to evaluate the sensitivity of the model to the parameters used during its creation. Among these were a large system with double the number of monomers, a high molecular weight system in which the number of chain initiating reactive monomers was limited to 10, and a uniform chain length system in which all chains were constrained to a uniform length. None of these alternative systems exhibited properties statistically different from the baseline. Preliminary results indicated, however, that the properties of the baseline systems were significantly different than experimental values. Polymers in general, and ionomers in particular, require long simulation times to relax to an equilibrium configuration. It was found that increasing the equilibration time from 1.0 ns to 20 ns was required to establish good clustering of the acid side groups, which is necessary to achieve a valid model to compare with experiments. Table 1 summarizes the differences between the baseline case and the well-equilibrated case. Further discussion of the causes of this equilibration time dependency is provided in the following section.

Finally, cubic simulation cells were found to be incompatible with the RNEMD simulations of viscosity and thermal conductivity. Achieving a smooth, steady-state gradient profile requires the use of a simulation cell that is elongated along one direction. A cell with relative dimensions of LxLx3L (L=46.5Å) was used in this work, and care was taken to ensure that the cell had the same total volume and density of that used in the cubic unit cell simulations.

RESULTS AND DISCUSSION

Structural Properties

Density is a convenient parameter for quickly assessing the quality of the force field used to study a polymeric system. For the systems considered in this work, including the variants with larger molecular weight and system size, the density is found not to vary significantly. For the systems equilibrated for 20

ns, the average density is 0.865 g/cc. This is within 10% of the experimental value of 0.95 g/cc measured for Surlyn® 8940.[18] In view of the substantial difference in molecular weight between the experimental and simulated materials, this magnitude of error is not unexpected. As seen in Table 1, there is little difference in density between the baseline case and the well-equilibrated system. So, while the predicted densities are in reasonably good agreement with experiment, they cannot be used as a metric for determining when the system has reached equilibrium.

While the density was found to be relatively insensitive to equilibration time, the stress-strain plots shown in Figure 2 reflect a significant change in mechanical behavior between the two systems. Specifically, increasing the equilibration time from 1 ns to 20 ns results in a near doubling of the elastic modulus, from 164 MPa to 325 MPa. The agreement of the well-equilibrated model with experiment is quite good, falling within 7% of the experimental bounds.[8a] Because of the short chain lengths and very high strain rates used in these simulations, this agreement with experiment is perhaps better than expected. Fortuitous cancellation of error cannot be excluded at this time and future simulations with much larger systems and slower strain rates will be required to confirm these results.

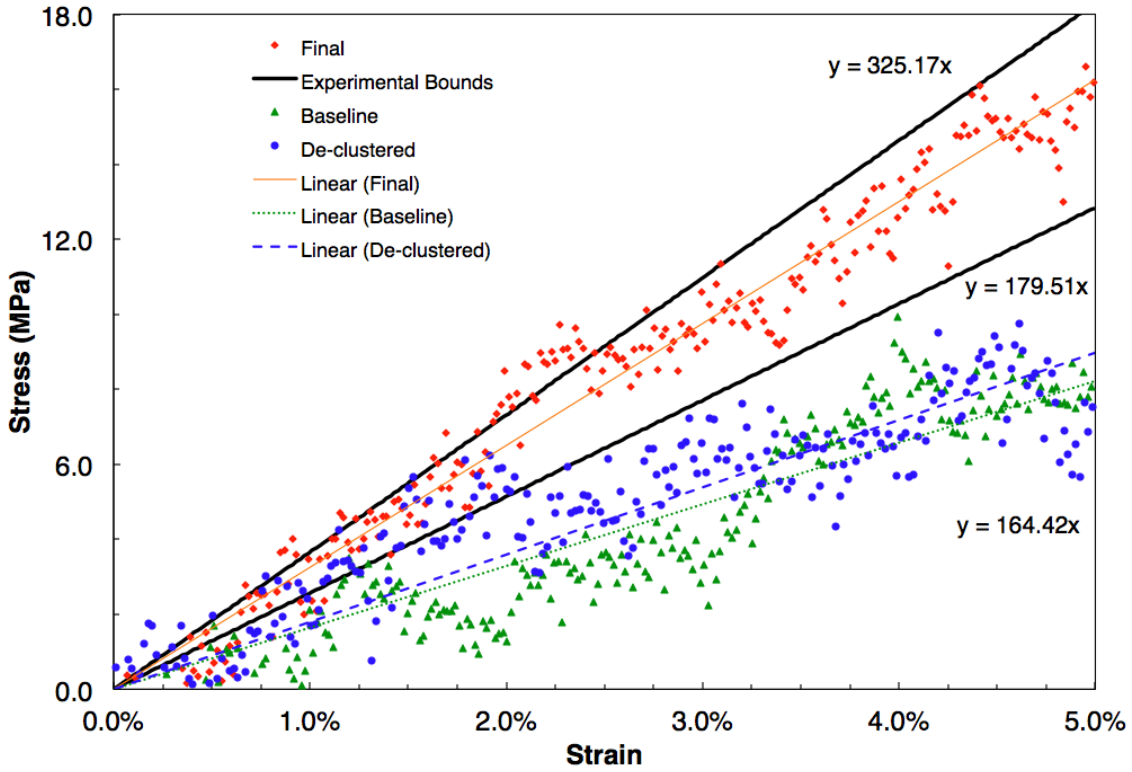

Figure 2. Stress-strain response of the well-equilibrated system (red diamonds), the baseline system (green triangles), and a de-clustered system (blue circles) along with the upper and lower experimental bounds (thick black lines). Also shown are the best fit lines for each system: well-equilibrated (red solid line), baseline (green dotted line), and de-clustered (blue dashed line).

There is broad consensus in the literature that clustering of the acid groups, in both the protonated and ionized forms, plays a critical role in both the self-healing behavior and mechanical properties of ionomers. To check if this clustering mechanism could help explain the significant difference in the tensile moduli calculated for the baseline and well-equilibrated systems, the radial distribution functions between pairs of carbonyl carbons were collected and are compared in Figure 3. These distributions were calculated by averaging the distribution of carbonyl carbon separations, measured during 1 ns simulations, starting from the baseline and well-equilibrated systems. The sharp, narrow peaks found in the RDF for the well-equilibrated system (solid line) indicate the presence of relatively structured clusters of carbonyl carbons in the 4-6 Å range. The broader, featureless peaks seen in plot for the baseline system

(dashed line) provide evidence that the baseline system has not had sufficient equilibration time to develop well-structured clusters.

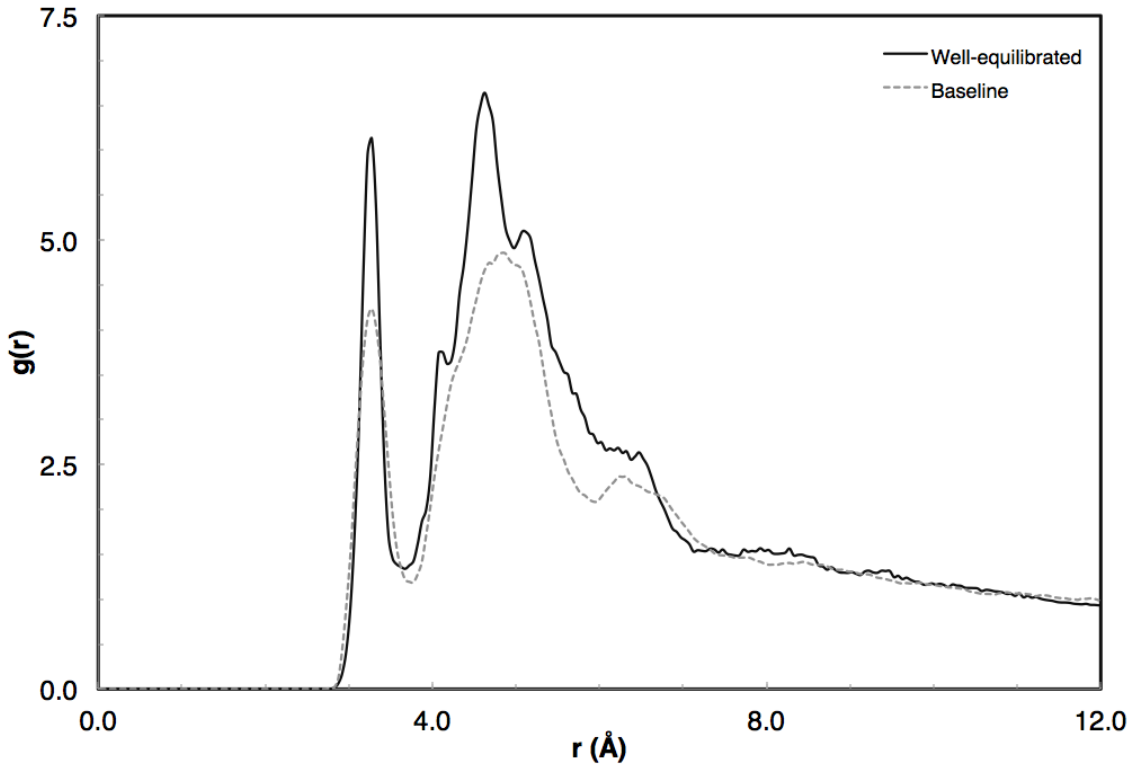

Figure 3. Radial distribution function between carbonyl carbons from a well-equilibrated system (solid black line) and the baseline system (dashed gray line).

To evaluate the thermal stability of the clusters, the well-equilibrated simulation cell was heated to 450 K, which is above the order-disorder transition temperature for the clusters, and then rapidly quenched to 300 K to lock in the disordered structure.[8a, 8b] The stress-strain curve for this system, shown in blue in Figure 2, is very similar to the curve of the baseline system and their moduli differ by only about 10%. Because the temperature ramp and quench were done too rapidly to permit large changes in polymer backbone configurations, this result supports the idea that the enhanced modulus is largely a result of ionic cluster formation rather than any other structural changes occurring during the longer equilibration.

Thermal Properties and Phase Behavior

Correctly modeling the thermal properties of this material is critical because self-healing is directly tied to the polymer's ability to melt and flow to heal the damage at the impact site. Heat capacity (C_p) and thermal expansion coefficient (α) are two thermodynamic properties that dictate how a material responds to an energy input, such as the heating resulting from compression and friction during a ballistic impact. Predicting these values from simulation also provides another point of validation for the model because experimental data are available for comparison. Using the methods described earlier, C_p is predicted to be 1.546 J/g-K for the baseline system and 1.746 J/g-K for the well-equilibrated system, compared to an experimental value of 1.850 J/g-K. The improved agreement with experiment found for the well-equilibrated system indicates that clustering has an important effect on heat capacity. This can be understood by considering the additional thermal energy input that is required to disrupt the ionic and hydrogen bonding in the clusters, which are absent in the baseline model system.[8b]

The values of α from the baseline system and the well-equilibrated system are 3.10×10^{-4} K^{-1} and 2.59×10^{-4} K^{-1}, respectively, compared to an experimental value of 2.094×10^{-4} K^{-1}. So, while the value calculated for the well-equilibrated system compares more favorably with experiment than the baseline system, the error is still about 20%. This may indicate that, as in the case of the predicted density, the much larger number of vdW interactions between polymer backbone carbon atoms dominates the volumetric behavior of the system. The resistance to expansion arising from the more strongly interacting cluster atoms is reflected in the lower α for the well-equilibrated system, relative to the baseline system.

It is also important that transition temperatures, which characterize the transition points between glassy, ordered, disordered, and melt states, be accurately predicted in simulations of self-healing materials. In Figure 4, calculated density is plotted as a function of simulation temperature, along with best fit lines for subsets of the data. The intersections of these best fit lines are identified as the transition temperatures.[19] The gradual change in slope over the range of temperatures considered is commonly

observed in simulations due to the limited system size and rapid heating rate.[20] To avoid biasing the transition temperatures found using this procedure, a number of fits to the data were performed. The number of best fit lines was varied between one and six, as was the number of data points allocated to each best fit line in each trial. The optimal number of segments and allocation of points to each segment were determined by a least-squares fitting procedure, using the combined R^2 values as the measure of quality of fit. The four segments and data point distribution shown in Figure 4 are the best outcome identified. As mentioned above, the temperatures at which these best fit lines intersect are taken to be the transition temperatures and are labeled on the graph for the well-equilibrated system and given in Table 1 for both simulated systems, along with the experimentally measured temperatures.

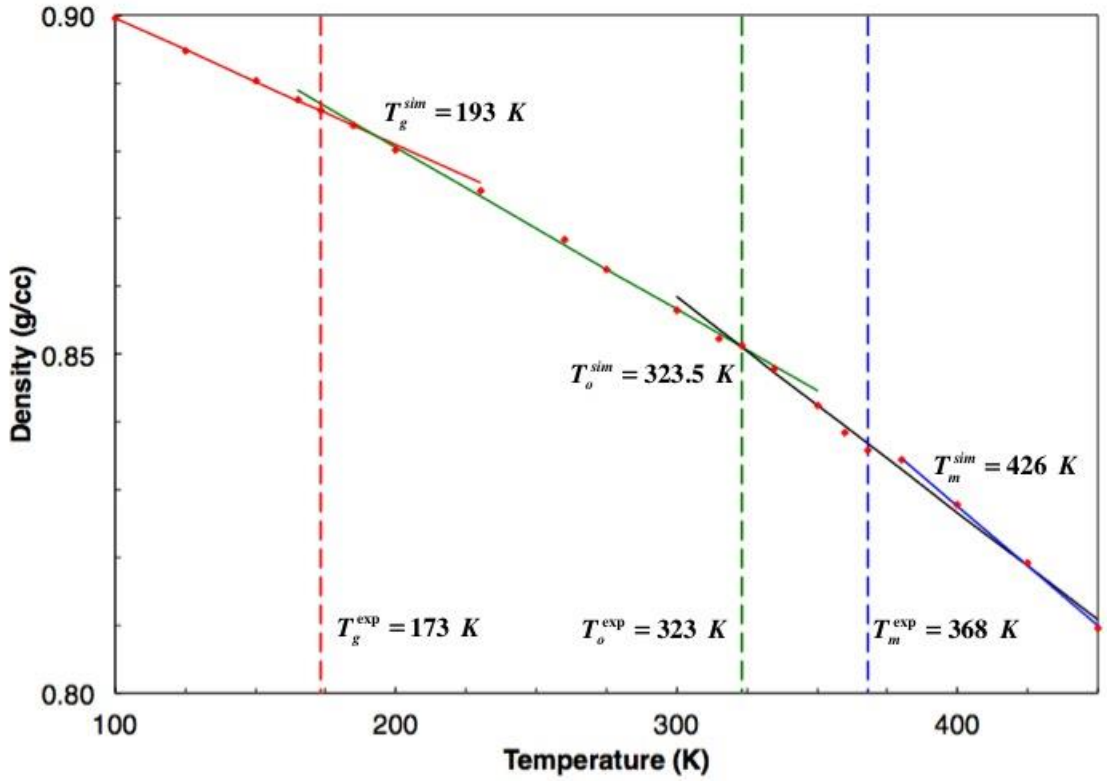

Figure 4. Transition temperature diagram showing the calculated densities (red diamonds) as a function of temperature. The fitted states (solid lines) are shown along with the experimental values (dashed lines) for transitions for clarity.

The vertical dashed lines in Figure 4 represent the experimental transition temperatures measured using DSC.[8b] The lines at 173 K, 323.5 K, and 368 K are associated with the glass transition, T_g, the cluster order-disorder transition, T_o, and the melting point, T_m, temperatures, respectively. The figure clearly shows that the simulation results for T_g (193 K) and T_m (426 K) are higher than the experimental values by 20 K and 58 K, respectively. The glass transition and melting are true thermodynamic phase transitions in the real material which are difficult to predict accurately with molecular dynamics simulations because of the system size and heating rate issues mentioned above. The order-disorder transition temperature on the other hand, agrees very well with the experimental result. This is likely due to the fact that the thermal disruption of the clusters is a much more local phenomenon that probes the structure and energetics of a relatively small group of atoms.

When the fitting procedure was repeated for the density-temperature data found in the baseline simulation, the best fit solution revealed that the data were better represented by three lines, rather than the four found for the well-equilibrated system. As shown in Table 1, this result indicates that baseline system exhibits glass transition and melting transitions, but not and order/disorder transition. This is consistent with earlier indications that clustering has not occurred during the short equilibration time used in the baseline system simulation. The disappearance of the order/disorder transition is also observed experimentally for samples that have been heated past the melting point and retested without allowing time for cluster reformation.[8b]

Table 1. Comparison of properties between baseline case, the well-equilibrated case, and the experimental measurements.

System	Density (g/cc)	Young's Modulus (MPa)	Heat Capacity (J/gK)	Thermal Expansion Coefficient (10^{-4} K^{-1})	T_g (K)	T_o (K)	T_m (K)	Thermal Conductivity (W/mK)
Baseline	0.853	164	1.546	3.1	178	N/A	335	0.19
Well-equilibrated	0.865	325	1.746	2.59	193	323.5	426	0.197
Experimental	0.95	320	1.85	2.09	173	323	368	0.155

Viscosity and Thermal Conductivity

The discussion to this point has focused on the static and quasi-static properties of Surlyn® 8940, but dynamic properties are critical in applications such as puncture healing. The rate and extent of thermal energy transfer away from the puncture site have a large effect on the structural state and elastic behavior of the material. Thermal conductivity is calculated by swapping the kinetic energy between pairs of atoms in different slices of the simulation cell to achieve a stable temperature gradient between opposing sides of the cell. Swaps are performed periodically to replicate the effect of applying a constant heat flux. The rate at which swaps are performed determines the rate of simulated heat flux. To examine the sensitivity of calculated properties to this rate, 1000, 2000, and 5000 steps between swaps were tested in this work. Figure 5 demonstrates that smooth gradients were achieved in each case, although their slopes differ. Using Fourier's Law, the thermal conductivity is determined by the ratio of total heat flux to the

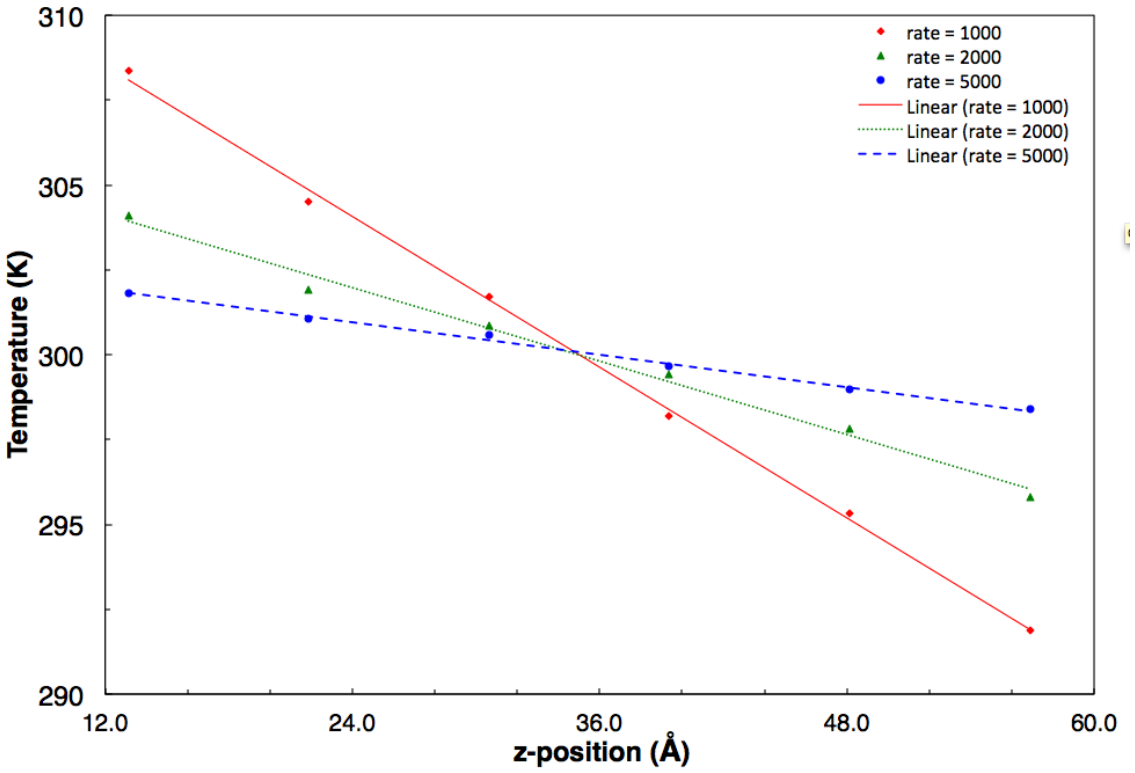

Figure 5. Temperature profiles at a swap rate of 1000 (red diamonds), 2000 (green triangles), and 5000 (blue circles) steps along with fitted lines.

temperature gradient established during the simulation. While the simulations with higher swap rates yielded higher thermal conductivities, the average over the rates used here is 0.197 W/mK. This result agrees reasonably well with the experimental value of 0.155 W/mK. Thermal conductivity was also calculated for the baseline system using the same procedure. The result, 0.190 W/mK, was very similar, indicating that cluster formation has a small effect on thermal conductivity.

Despite the reasonable results obtained by use of the RNEMD procedure for calculating thermal conductivity, applying it to the calculation of viscosity for this polymer system was unsuccessful. After attempting swap rates of 2, 10, 100, and 1000 with a 1 fs time step, it was found that only the fastest rate, or equivalently the highest shear rate, was able to produce a stable velocity gradient. The viscosity found using this rate was about three orders of magnitude below the experimental value of approximate 13,000 poise.[8a] Although this method can work well for lower molecular weight fluids, the bonding and entanglements found in the present system produce a strong resistance to changes in momentum, making it very difficult to attain a steady-state flux with a reasonable swap rate. Further work will be required to establish a reliable means for predicting the viscosity of this system.

CONCLUSIONS

Understanding the behavior of self-healing materials at the molecular level is essential to the process of tailoring their properties or designing new polymers with the ability to self-heal. The model of Surlyn® 8940 developed in this work is a first step in that direction and has been shown to produce reasonably good results with respect to the mechanical and thermal properties. As is almost always true of molecular simulations of macroscopic materials, the results obtained using this model and the simulation procedures described above could be improved by increasing the duration and size of the simulations at the cost of greater computational expense.

While reproducing the results of experimental measurements is important in validating the model, the real value of simulations of this type lies in providing physical insight into the mechanisms that lead to the desirable behavior of the material. The existence of clusters of ionic or hydrogen bonded groups has

long been thought to play a role in the self-healing phenomena, but it has been difficult to prove experimentally. As demonstrated in this work, analysis of simulation results can provide a molecular level perspective on this behavior and support the hypothesis that well-established cluster networks drive many thermal and mechanical properties found in self-healing polymer materials.

In a sense, this system may be viewed as a multi-phase system comprised of nanoscale clusters acting as filler 'particles' cross-linked to the matrix polymer. Rather than exhibiting brittle failure, as is often found in multi-phase systems the material maintains strength due to the dynamic process of ionic and hydrogen bond formation and breakage. While the yield and failure processes were beyond the scope of the present work, they are clearly of interest. Some interesting results in this area may be found in the work of Varley and van der Waag, who experimentally studied the effect of adding small molecule dicarboxylic acids to Surlyn® 8940.[8d] They found that these additives extended the elastic region, while reducing the elastic modulus due to plasticization. Results such as these motivate the future extension of this work to enable computationally guided design of new and more efficient self-healing materials for a range of applications where damage tolerance and resilience are enabling properties.

REFERENCES

1. (a) Wool, R. P., Self-healing materials: A review. *Soft Matter* 2008, *4*, 400; (b) Wu, D. Y.; Meure, S.; Solomon, D., Self-healing polymeric materials: A review of recent developments. *Prog. Polym. Sci.* 2008, *33*, 479; (c) Murphy, E. B.; Wudl, F., The world of smart healable materials. *Prog. Polym. Sci.* 2010, *35*, 223; (d) Syrett, J. A.; Becer, C. R.; Haddleton, D. M., Self-healing and self-mendable polymers. *Polym. Chem.* 2010, 7, 978.
2. (a) White, S. R.; Sottos, N. R.; Geubelle, P. H.; Moore, J. S.; Kessler, M. R.; Sriram, S. R.; Brown, E. N.; Viswanathan, S., Autonomic healing of polymer composites. *Nature* 2001, *409* (6822), 794; (b) Brown, E. N.; Sottos, N. R.; White, S. R., Fracture testing of a self-healing polymer composite. *Exp. Mech.* 2002, *42*, 372; (c) Brown, E. N.; White, S. R.; Sottos, N. R., Fatigue crack propagation in microcapsule-toughened epoxy. *J. Mater. Sci.* 2006, *41*, 6266; (d) Kessler, M. R.; Sottos, N. R.; White, S. R., Self-healing structural composite materials. *Compos. Pt. A-Appl. Sci. Manuf.* 2003, *34*, 743; (e) Toohey, K. S.; Sottos, N. R.; Lewis, J. A.; Moore, J. S.; White, S. R., Self-healing materials with microvascular networks. *Nat. Mater.* 2007, *6*, 581.
3. (a) Dry, C., Passive tunable fibers and matrices. *Int. J. Mod. Phys. B* 1992, *6*, 2763; (b) Dry, C., Procedures developed for self-repair of polymer matrix composite materials. *Compos. Struct.* 1996,

35, 263; (c) Dry, C.; McMillan, W., Three-part methylmethacrylate adhesive system as an internal delivery system for smart responsive concrete. *Smart Mater. Struct.* 1996, *5*, 297.

4. Hager, M. D.; van der Zwaag, S.; Schubert, U. S., *Self-Healing Materials*. 1 ed.; Springer International Publishing: Switzerland, 2016.

5.(a) John, M.; Li, G. Q., Self-healing of sandwich structures with a grid stiffened shape memory polymer syntactic foam core. *Smart Mater. Struct.* 2010, *19*, 075013; (b) Meure, S.; Furman, S.; Khor, S., Polyethylene-co-(methacrylic acid) healing agents for mendable carbon fiber laminates. *Macromol. Mater. Eng.* 2010, *295*, 420; (c) Nji, J.; Li, G. Q., A self-healing 3D woven fabric reinforced shape memory polymer composite for impact mitigation. *Smart Mater. Struct.* 2010, *19*, 035007; (d) Roy, N.; Bruchmann, B.; Lehn, J.-M., DYNAMERS: dynamic polymers as self-healing materials. *Chem. Soc. Rev.* 2015, *44*, 3786.

6. (a) Chen, X. X.; Wudl, F.; Mal, A. K.; Shen, H. B.; Nutt, S. R., New thermally remendable highly cross-linked polymeric materials. *Macromolecules* 2003, *36*, 1802; (b) Park, J. S.; Darlington, T.; Starr, A. F.; Takahashi, K.; Riendeau, J.; Hahn, H. T., Multiple healing effect of thermally activated self-healing composites based on Diels-Alder reaction. *Compos. Sci. Technol.* 2010, *70*, 2154; (c) Chen, X. X.; Dam, M. A.; Ono, K.; Mal, A.; Shen, H. B.; Nutt, S. R.; Sheran, K.; Wudl, F., A thermally re-mendable cross-linked polymeric material. *Science* 2002, *295*, 1698.

7. (a) Cordier, P.; Tournilhac, F.; Soulie-Ziakovic, C.; Leibler, L., Self-healing and thermoreversible rubber from supramolecular assembly. *Nature* 2008, *451*, 977; (b) Montarnal, D.; Cordier, P.; Soulie-Ziakovic, C.; Tournilhac, F.; Leibler, L., Synthesis of self-healing supramolecular rubbers from fatty acid derivatives, diethylenetriamine, and urea. *J. Polym. Sci. Pol. Chem.* 2008, *46*, 7925; (c) Montarnal, D.; Tournilhac, F.; Hidalgo, M.; Couturier, J. L.; Leibler, L., Versatile one-pot synthesis of supramolecular plastics and self-healing rubbers. *J. Am. Chem. Soc.* 2009, *131*, 7966.

8. (a) Gordon, K., Bogert, P., Howell, P., Burke, E., Cramer, E., Yost, W.T., and Siochi, E., "Ballistic Puncture Self-healing Polymeric Materials." NASA/TM–2017-219642; (b) Kalista, S. J.; Ward, T. C., Thermal characteristics of the self-healing response in poly (ethylene-co-methacrylic acid) copolymers. *J. R. Soc. Interface* 2007, *4*, 405; (c) Kalista, S. J.; Ward, T. C.; Oyetunji, Z., Self-healing of poly(ethylene-co-methacrylic acid) copolymers following projectile puncture. *Mech. Adv. Mat. Struc.* 2007, *14*, 7; (d) Varley, R. J.; Shen, S.; van der Zwaag, S., The effect of cluster plasticisation on the self healing behaviour of ionomers. *Polymer* 2010, *51*, 679; (e) Varley, R. J.; van der Zwaag, S., Towards an understanding of thermally activated self-healing of an ionomer system during ballistic penetration. *Acta Mater.* 2008, *56*, 5737; (f) Varley, R. J.; van der Zwaag, S., Development of a quasi-static test method to investigate the origin of self-healing in ionomers under ballistic conditions. *Polym. Test* 2008, *27*, 11; (g) Varley, R. J.; van der Zwaag, S., Autonomous damage initiated healing in a thermo-responsive ionomer. *Polym. Int.* 2010, *59*, 1031.

9. Plimpton, S., Fast parallel algorithms for short-range molecular dynamics. *J. Comput. Phys.* 1995, *117*, 1.

10. Hoover, W. G., Canonical dynamics: Equilibrium phase-space distributions. *Phys. Rev. A* 1985, *31*, 1695.

11. Allen, M. P.; Tildesley, D. J., *Computer Simulation of Liquids*. Clarendon Press: Oxford, 1987.

12. (a) Muller-Plathe, F., Reversing the perturbation in nonequilibrium molecular dynamics: An easy way to calculate the shear viscosity of fluids. *Phys. Rev. E* 1999, *59*, 4894; (b) Muller-Plathe, F.; Reith, D., Cause and effect reversed in non-equilibrium molecular dynamics: An easy route to transport coefficients. *Comput. Theor. Polym. Sci.* 1999, *9*, 203.

13. Mayo, S. L.; Olafson, B. D.; Goddard, W. A., DREIDING: A generic force-field for molecular simulations. *J. Phys. Chem.* 1990, *94*, 8897.

14. Vanommeslaeghe, K.; Hatcher, E.; Acharya, C.; Kundu, S.; Zhong, S.; Shim, J.; Darian, E.; Guvench, O.; Lopes, P.; Vorobyov, I.; MacKerell, A. D., CHARMM General force field: a force field for drug-like molecules compatible with the charmm all-atom additive biological force fields. *J. Comput. Chem.* 2010, *31*, 671.

15. Hadley, K. R.; McCabe, C., A coarse-grained model for amorphous and crystalline fatty acids. *J. Chem. Phys.* 2010, *132*, 134505.

16. Perez, M.; Lame, O.; Leonforte, F.; Barrat, J. L., Polymer chain generation for coarse-grained models using radical-like polymerization. *J. Chem. Phys.* 2008, *128*, 234904.

17. Farah, K.; Karimi-Varzaneh, H. A.; Muller-Plathe, F.; Bohm, M. C., Reactive molecular dynamics with material-specific coarse-grained potentials: Growth of polystyrene chains from styrene monomers. *J. Phys. Chem. B* 2010, *114*, 13656.

18. DuPont Surlyn® Resins Product Data Sheet.

19. Fox, T. G.; Loshaek, S., Influence of molecular weight and degree of crosslinking on the specific volume and glass temperature of polymers. *J. Polym. Sci.* 1955, *15*, 20.

20. Varshney, V.; Patnaik, S. S.; Roy, A. K.; Farmer, B. L., A molecular dynamics study of epoxy-based networks: cross-linking procedure and prediction of molecular and material properties. *Macromolecules* 2008, *41*, 6837.

REPORT DOCUMENTATION PAGE

Form Approved
OMB No. 0704-0188

1. REPORT DATE *(DD-MM-YYYY)*
1-07-2020

2. REPORT TYPE
Technical Memorandum

3. DATES COVERED *(From - To)*

4. TITLE AND SUBTITLE

The Influence of Acid Group Clustering on the Thermal and Mechanical Properties of a Self-Healing Polymer

5a. CONTRACT NUMBER

5b. GRANT NUMBER

5c. PROGRAM ELEMENT NUMBER

6. AUTHOR(S)

Keith L. Gordon; Kristopher E. Wise; Emilie J. Siochi; Kevin R. Hadley

5d. PROJECT NUMBER

5e. TASK NUMBER

5f. WORK UNIT NUMBER
561581.02.08.07.43.01

7. PERFORMING ORGANIZATION NAME(S) AND ADDRESS(ES)

NASA Langley Research Center
Hampton, VA 23681-2199

8. PERFORMING ORGANIZATION REPORT NUMBER

9. SPONSORING/MONITORING AGENCY NAME(S) AND ADDRESS(ES)

National Aeronautics and Space Administration
Washington, DC 20546-0001

10. SPONSOR/MONITOR'S ACRONYM(S)
NASA

11. SPONSOR/MONITOR'S REPORT NUMBER(S)
NASA-TM-2020-5003983

12. DISTRIBUTION/AVAILABILITY STATEMENT

Unclassified
Subject Category : Nonmetallic Materials
Availability: NASA STI Program (757) 864-9658

13. SUPPLEMENTARY NOTES

14. ABSTRACT

To better understand the molecular level mechanisms behind the self-healing of polymersystems, this work developed and validated a molecular dynamics model for a self-healing polymer, Surlyn®8940. The polymer chains were built using free-radical polymerization between ethylene monomers (~95 mol%) and methacrylic acid monomers. Predicted thermal and structural properties includingthermal conductivity, heat capacity, transition temperatures, thermal expansion coefficient, density, and Young's modulus were shown to be in good agreement with experimental values.Furthermore, the effects of cluster formation amongthe acid groups on these properties were explicitly explored.

15. SUBJECT TERMS

self-healing polymer; computational modeling; simulation

16. SECURITY CLASSIFICATION OF:			17. LIMITATION OF ABSTRACT	18. NUMBER OF PAGES	19a. NAME OF RESPONSIBLE PERSON
a. REPORT	b. ABSTRACT	c. THIS PAGE			STI Help Desk (email: help@sti.nasa.gov)
U	U	U	UU	25	19b. TELEPHONE NUMBER *(Include area code)* (757) 864-9658